Journal of Physics D: Applied Physics

PAPER

Gate-polarity-dependent doping effects of H_2O adsorption on graphene/SiO_2 field-effect transistors

To cite this article: Mengjian Xu *et al* 2020 *J. Phys. D: Appl. Phys.* **53** 455301

View the article online for updates and enhancements.

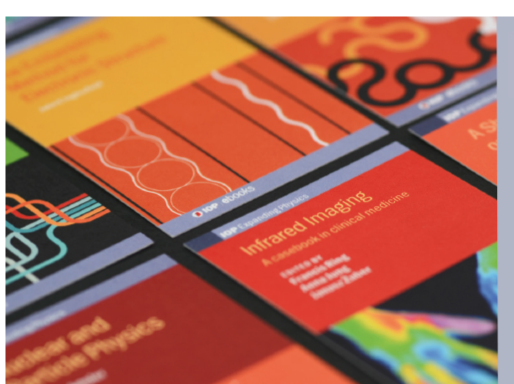

IOP ebooks™

Bringing together innovative digital publishing with leading authors from the global scientific community.

Start exploring the collection–download the first chapter of every title for free.

This content was downloaded from IP address 202.120.209.41 on 02/11/2020 at 07:54

IOP Publishing Journal of Physics D: Applied Physics
J. Phys. D: Appl. Phys. 53 (2020) 455301 (7pp) https://doi.org/10.1088/1361-6463/aba70d

Gate-polarity-dependent doping effects of H_2O adsorption on graphene/SiO_2 field-effect transistors

Mengjian Xu[1,2], Xuguang Guo[1], Lin Chen[1], Anqi Yu[1,3], Xingeng Zhou[1], Hao Wang[2], Yue Gu[2], Fang Wang[2] and Yiming Zhu[1,3]

[1] Shanghai Key Lab of Modern Optical System, Terahertz Technology Innovation Research Institute, Terahertz Spectrum and Imaging Technology Cooperative Innovation Center, University of Shanghai for Science and Technology, 516 Jungong Road, Shanghai 200093, People's Republic of China
[2] State Key Laboratory of Infrared Physics, Shanghai Institute of Technical Physics, Chinese Academy of Sciences, 500 Yutian Road, Shanghai 200083, People's Republic of China
[3] Shanghai Institute of Intelligent Science and Technology, Tongji University, Shanghai 200092, People's Republic of China

E-mail: xgguo@usst.edu.cn, fwang@mail.sitp.ac.cn and ymzhu@usst.edu.cn

Received 28 April 2020, revised 5 July 2020
Accepted for publication 17 July 2020
Published 11 August 2020

Abstract

Due to its huge surface-to-volume ratio, graphene has become one of the most popular materials for sensors. However, H_2O molecules in atmospheric environments can cause the instability of graphene devices, which greatly limits the practical applications of graphene devices. The charge transfer between graphene and adsorbed H_2O molecules has been proved previously by first-principle studies, but experimental demonstrations are still lacking. Here, gate-polarity-dependent doping behaviors of adsorbed H_2O molecules on a graphene/SiO_2 field-effect transistor (GFET) are experimentally investigated. The results indicate that the orientation of the adsorbed H_2O can be affected by the gate-voltage polarity due to the dipolar interaction, which leads to the amphoteric doping behavior of adsorbed H_2O molecules. With reducing the graphene layer number, the amphoteric doping behavior is more sensitive to the gate voltage polarity. Our results are helpful for constructing high performance graphene-based sensors and enhancing the stability of GFETs.

Keywords: graphene, water molecule adsorption, gate-polarity

(Some figures may appear in colour only in the online journal)

1. Introduction

Due to the in-planar sp2 σ and out-planar π C-C bonds and the two-dimensional (2D) honeycomb crystal structure, graphene has many unique properties, such as good chemical stability, strong mechanical strength, high thermal conductivity, gapless Dirac energy–momentum dispersion relation, ultra-high carrier mobility, electrically-tunable Fermi energy, and huge surface-to-volume ratio [1, 2]. All these features of graphene are suitable for constructing high performance sensors [3]. Since the demonstration of single-molecule sensing ability of graphene-based devices [4], there are many investigations on the adsorption mechanisms of graphene. Notably, adsorption mechanisms of small molecules (NH_3, NO_x, CO, O_2, and H_2O, etc), organic molecules, and biomolecules on graphene and other 2D materials were theoretically studied based on density functional theory and molecular dynamics theory [3, 5–9]. In the experimental aspect, several optical spectral techniques, such as absorption, Raman, and photoluminescence are used to character the bonds between adsorbates and the 2D materials [3, 10]. More directly, the micro morphologies of adsorbates on 2D surfaces are observed by using atom force microscopy (AFM), scanning tunneling microscopy, and Kelvin probe force microscopy

 © 2020 IOP Publishing Ltd Printed in the UK

[11–14]. Many sensors based on the adsorption of molecules on graphene and other 2D materials are realized and proposed [3, 14–16].

Previous investigations show that the adsorbed H_2O molecules on graphene behave as acceptors [4–6]. By utilizing this property, graphene/SiO_2 field-effect transistor (GFET)-based fast response/recovery humidity sensors can be constructed [3, 5, 6, 14]. On the other hand, the adsorption of H_2O molecules will change the electrical properties of GFET working in atmospheric conditions. Many investigations on the adsorption mechanism of H_2O molecule and the doping behaviors were performed [17–19], such as interactions between H_2O molecules and defects, edges, and substrates. Adsorption/desorption experiments indicate that there are no chemical bonds between the adsorbed H_2O molecules and the carbon atoms located at the periodic honeycomb cites, and the adsorption is through the Van der Waals (VdW) force [3]. Because of the weak VdW interaction (a binding energy of ~100 meV), few-layer graphene between the adsorbed polar molecules and substrates cannot effectively screen the dipolar interactions between them [16, 20]. Theoretical calculations [7, 8] based on density functional theory show that for a perfect and free-standing mono-layer graphene, the effects of adsorbed H_2O molecules on the electrical properties of graphene are negligible. Moreover, H_2O-adsorption-induced doping behaviors can be attributed to the interaction of the H_2O molecules and the substrate. For example, for a SiO_2 substrate, the local electric field introduced by adsorbed H_2O molecules will change the energy position of SiO_2 impurity band [8], which results in the doping behavior of H_2O adsorption. The doping type is dependent on the orientation of the adsorbed H_2O molecules. For polar NH_3 molecules, an amphoteric doping behavior is found originating from the different adsorption orientations [5, 6]. Theoretical calculations predicted that the adsorption of H_2O on graphene should show the similar amphoteric doping effect. However, no such amphoteric doping behavior was found in recent experiments [3].

In this paper, we report a gate-polarity-induced amphoteric doping behavior of H_2O molecules adsorption on GFETs within a 15-min time scale, in atmospheric conditions with different relative humidities (RHs), and at room temperature (300 K). Mechanically exfoliated multilayer (4.5 nm thick, ~12 layers) graphene is used to fabricate the back-gated GFET on a SiO_2/p-Si substrate with p denoting the hole doping. Zero, positive, and negative gate voltages are respectively applied to the GFET in atmospheric conditions with 0% RH (dry air), 58% RH, and 100% RH for 30 min. In comparison with the case of zero gate voltage, the charge neutral point (CNP) in the transfer curve shifts to right for positive gate voltage and to left for negative gate voltage, which indicates that a portion of the adsorbed H_2O molecules acts as acceptors with a positive gate voltage applied. The hole doping of H_2O adsorption on GFET/SiO_2 is attributed to the dipolar-interaction-induced change of orientation of the adsorbed H_2O molecules. The amphoteric doping behavior is more sensitive to the gate voltage polarity when the graphene layer number is reduced. Our main experimental findings are in accordance with theoretical calculations [7, 8].

2. Device fabrication and drift-diffusion model

The schematic and the micro-photograph of the GEFT are shown in figures 1(a) and (b), respectively. The multilayer graphene channel is mechanically exfoliated from a bulk highly ordered pyrolytic graphite by scotch tape onto a substrate of 300 nm SiO_2 over a heavily p-doped Si (500 μm) substrate. The transfered graphene flakes are characterized by using optical microscopy, Raman spectroscopy, and AFM. The electrodes of the GFET are made with standard e-beam lithographic technology, and the photoresist used in the electron beam lithography is polymethyl-methacrylate (PMMA). Then a Cr/Au film (5/60 nm) is deposited with a thermal evaporation process. Finally, the standard lift-off process is used to remove the excess metal film. To remove the PMMA and the tape residues, water, and other adsorbates, thermal annealing is performed at 473 K for 120 min at a low atmospheric pressure of 156 Pa. After annealing, the CNP on the transfer curve shifts from $V_g = 25$ V to $V_g = 5$ V, which indicates that the graphene channel is weakly p-doped and most of the residues are removed. As shown in figure 1(b), the graphene channel is around 2.5 μm wide and 5.0 μm long between every two nearest-neighbor contacts. In order to confirm the layer number of graphene, the Raman spectrum of the GFET is measured with a 532 nm excitation laser. The peak intensities of G band (~1580 cm^{-1}) and 2D band (~2750 cm^{-1}) are shown in figure 1(c). The higher G-band intensity indicates that the graphene is multilayer [21]. For further determining the thickness of the graphene channel, the thickness profile as shown in the inset of figure 1(b) is acquired by using a AFM (Bruker multimode 8). The thickness of the graphene channel is around 4.5 nm, which indicates that the layer numbers of graphene are about 12 layers. The finished device was mounted and wire-bonded to a PCB sample holder. In figure 1(d), the linear output characteristics of the GFET measured at $V_g = 0$ V indicates that the contacts between graphene and metal are Ohmic. The linear output characteristics is kept at different gate voltages (not shown). In order to investigate the adsorption of H_2O molecules, the device is mounted into a home-made vacuum chamber, in which the ambient environment can be well controlled. To characterize the performance of the GFET, the basic electrical properties including the source-drain current–voltage curves (I_d–V_d) and the transfer curves (I_d-V_g) with a fixed source drain bias voltage of 0.1 V are measured. A Keithley 2400 and an Agilent U3606A source-measurement units are utilized to record the data.

A drift–diffusion carrier transport model for graphene is used to evaluate the device parameters, including CNP, carrier mobility, and residual carrier concentration, by fitting the experimental transfer curves in different atmospheric conditions. The drift–diffusion carrier transport model for graphene can be formulated as

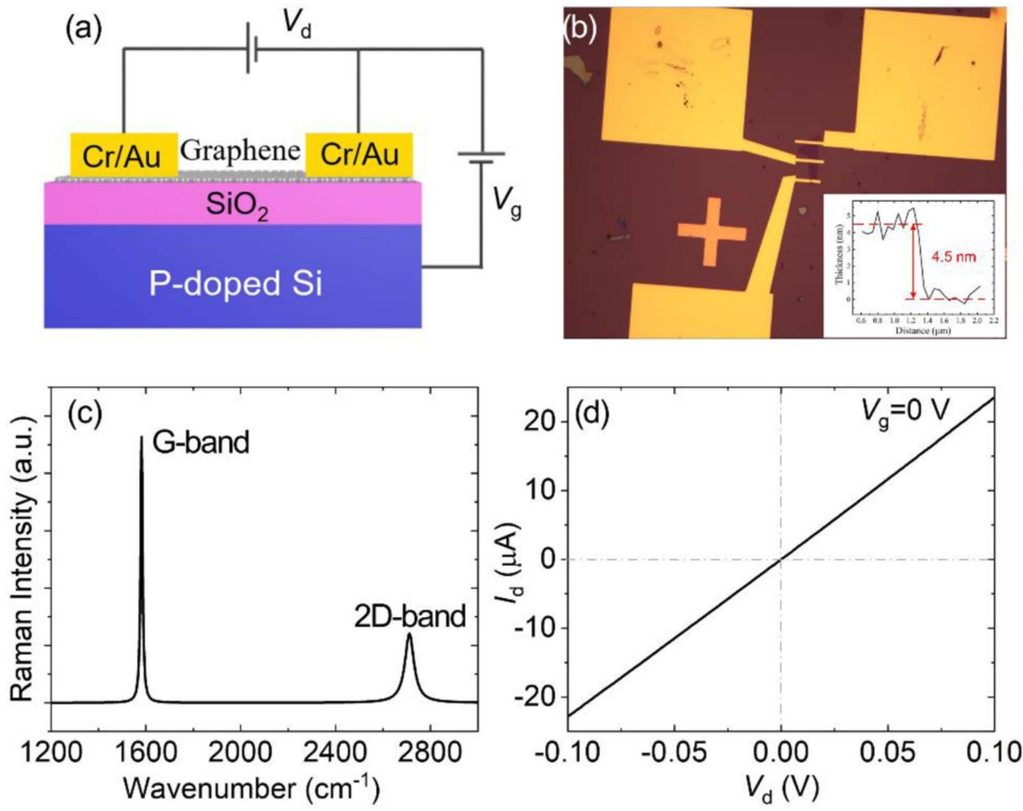

Figure 1. Schematic (a) and micro photograph (b) of the back gated GFET/SiO_2 with the inset shows the AFM thickness profile of graphene channel, (c) the Raman spectrum of graphene channel, and (d) the output characteristic of the GFET at $V_g = 0$ V.

$$
\begin{aligned}
&I_d = \frac{V_d}{R_{\text{tot}}}, C_{OX} = \frac{e_0 e}{d}, \\
&R_{\text{tot}} = R_c + R_{gr}, \\
&R_{gr} = \frac{L}{W}\sigma^{-1} = \frac{L}{W}\frac{1}{n_{\text{tot}} e \mu}, \\
&n_{\text{tot}} = \sqrt{n_0^2 + [n(V_g - V_{CNP})]^2}, \text{ and} \\
&V_g - V_{CNP} = \frac{ne}{C_{OX}} + \text{sgn}(n)\frac{\hbar v_F \sqrt{\pi |n|}}{2e},
\end{aligned} \tag{1}
$$

where I_d and $V_d = 0.1$ V are the source-drain current and the bias voltage. R_{tot}, R_c, and R_{gr} are the total resistance, the electrode–graphene contact resistance, and the graphene channel resistance, respectively. C_{OX}, ε, and d are the capacitance, dielectric constant, and thickness of SiO_2 gate layer, respectively. L and W represent the length and width of graphene channel. n_{tot}, n_0, and n are the total, residual, and gate-tunable carrier concentrations, respectively. σ, e, and μ are the conductivity, electron charge, and carrier mobility, respectively. V_g and $V_{CNP} = 0$ V are the gate voltage and the potential of Dirac point of graphene, respectively. $\hbar$ is the reduced Planck constant. $v_F = 10^6$ m s^{-1} is the Fermi velocity of graphene. The values of function are sgn(n) = 1 for n doping and sgn(n) = −1 for p doping. In equation (1), R_c, n_0, and μ are fitting parameters. The value of R_c is set to 700 Ω for all the different atmospheric conditions.

3. Electrical properties of the GFET/SiO_2 in different atmospheric conditions

The GFET is mounted in a dark vacuum chamber before each measurement to eliminate the influence of photo-gating effect, and the device is kept for 30 min at 7×10^{-4} Pa with zero V_d and V_g. The value of V_d is set to 0.1 V for all the measurements. As shown in figure 2, the electrical properties are firstly measured in vacuum condition (7×10^{-4} Pa, the same as below). Figure 2(a) shows the source-drain currents with respect to time at the gate voltages $V_g = 20$ V (a-1) and $V_g = -20$ V (a-2), respectively. A slight decrease of I_d (<0.25 μA, 1.2%) with time is observed at $V_g = 20$ V, and the variation of I_d at $V_g = -20$ V is negligible, which indicates that there are no gate-voltage-dependent carrier trapping/de-trapping related to SiO_2 substrate and adsorption/desorption processes at the time scale of ~15 min. Figure 2(b) shows the I_d–V_g curves measured in vacuum after the gate voltages $V_g = 0$ V, 20 V and −20 V being applied to the device for 30 min, respectively. Our experimental data show that such a time scale (30 min) is long enough for the GFET to reach a steady state. The three transfer I_d–V_g curves nearly overlap and the CNPs locate at about $V_g = -1.25$ V, which means the graphene channel is weakly n doped. No hysteresis is observed on the I_d–V_g curves for all the cases [22]. The details near the CNPs are shown in the inset of figure 2(b). In the case $V_g = 0$ V, the residual

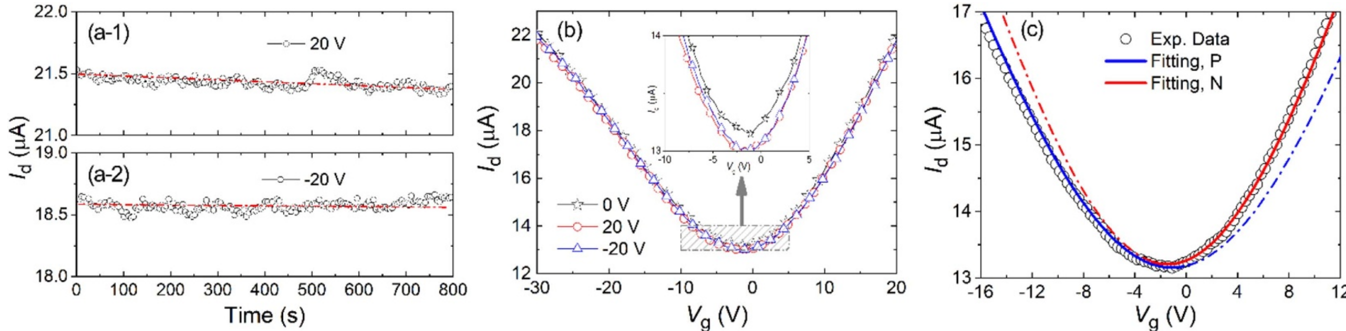

Figure 2. Electrical properties of the GFET/SiO_2 in vacuum. (a) Dependences of source-drain currents on time for gate voltages of 20 V (a-1) and −20 V (a-2) at a source-drain bias voltage of 0.1 V. The open circular scatters are experimental data, and the red point-dash lines are the fitting curves. Before each of the two measurements, the device is kept in vacuum, at zero source-drain bias voltage, and at zero gate voltage for 30 min. (b) Transfer curves of the GFET measured at once when the measurements of the corresponding current–time curves shown in (a) are finished. The inset is the transfer curves near the CNPs. (c) Theoretical fitting results based on the drift–diffusion model. Two sets of parameters are used to fit the experimental data at the two sides of the CNP, where P and N denote that hole and electron are the dominant carriers, respectively.

carrier concentration is a little higher than those in the other two cases, which may be contributed to the defects in SiO_2 substrate [23, 24]. As shown in figure 2(c), the transfer curve for $V_g = 0$ V is fitted by using equation (1) with fitting parameters $n_0 = 1.31 \times 10^{12}$ cm^{-2} and $\mu = 2410$ cm^2/(Vs) for holes (P section) and $\mu = 2460$ cm^2/(Vs) for electrons (N section). A weak asymmetry exists between the subsections right (electron) and left (hole) to the CNP, which is due to the different scattering rates for electrons and holes originating from the interface ionized scatters related to the SiO_2 substrate [25, 26].

The effects of H_2O adsorption on the electrical properties of the GFET are shown in figure 3. Before each measurement, the device is kept in dry air, 58% RH, and 100% RH atmospheric environments, respectively, with $V_d = 0$ V and $V_g = 0$ V for 30 min to make the GFET return to its initial state. The variations of I_d with respect to time at the fixed gate voltages $V_g = 20$ V (a-1) and $V_g = -20$ V (a-2) in different ambient environments are presented in figure 3(a). To clearly show the variations of I_d with time, different constant values of current are subtracted from the originate data and then all the I_d-time curves can be presented in the same panel with a much smaller current range. In dry air (0% RH), the values of I_d are nearly unchanged for $V_g = -20$ V and a slight decrease with time for $V_g = 20$ V. However, when the GFET is in the 58% RH and 100% RH atmospheric conditions, remarkable decreases of I_d with time are observed, and the decrease for the case of 100% RH is larger than that for the case of 58% RH. The above results indicate that the variations of I_d with respect to time is related to the gate-dependent H_2O adsorption on the graphene channel. In order to further explore the behaviors of gate-dependent H_2O adsorption, the transfer curves of the GFET with different gate voltages $V_g = 0$ V, −20 V, and 20 V are measured and the data are shown in figure 3(b). Before each gate-voltage sweeping, the device is in the corresponding atmospheric condition and with the corresponding gate voltage for 30 min. In dry air (figure 3(b-1)), due to the O_2-adsorption-induced p doping [6], the CNPs shift from $V_g = -1.25$ V (figure 2(a)) to $V_g = 6.5$ V for all the three cases of fixed gate voltages. The transfer curves are independent on the fixed gate voltages, which indicates that the adsorption/desorption processes of O_2 molecule on graphene are not affected by the gate voltage and this result is consistent with that shown in figure 3(a). However, in humid environments, the transfer curves are effectively changed by the fixed gate voltages. In the case of $V_g = 0$ V, the CNPs shift to $V_g = -3.0$ V for 58% RH and $V_g = -10.0$ V for 100% RH. In comparison with the I_d–V_g curves in dry air (figure 3(b-1)), for graphene, the effect of H_2O-induced n doping is stronger than that of O_2-induced p doping. At the same time, it can be found that the fixed positive gate voltage (red dash lines in figures 3(b-2) and (b-3)) leads to the right shift of the CNPs. On the contrary, the fixed negative gate voltage (blue dot-dash lines in figures 3(b-2) and (b-3)) leads to the left shift of the CNPs. In other words, the H_2O-adsorption-induced n doping can be reduced by applying positive gate voltages and enhanced by applying negative gate voltages. Therefore, the decreases of I_d with time in humidity environments shown in figure 3(a) originate from the gate-voltage-induced shifts of CNP.

To investigate the effects of graphene channel thickness, a GFET with a few-layer graphene channel (~1.0 nm thick, obtained from the AFM measurement (inset of figure 4(a))) is fabricated. As shown in figure 4(a), the linear I_d–V_d curve indicates the metal–graphene contacts are Omhic. Figure 4(b) shows that compared to the GFET with multilayer graphene channel, the few-layer GFET is more sensitive to the adsorbed H_2O molecules. In the atmospheric condition with 58% RH, the initial CNP shifts from 5.6 V to 19.6 V and 5.6 V to −6.8 V after continuously applying positive 20 V and negative 20 V gate voltages for 15 min, respectively. As shown in figure 4(c), in vacuum condition, the CNP of the few-layer GFET has no obvious change with the different gate voltages applied for 15 min. The slight shift of the CNP is due to the trap centers in the SiO_2 substrate [22]. Further, as shown in figure 4(d), the hysteresis of the transfer curves in the few-layer GFET in vacuum condition identifies the charge capture into and release from the trap centres in the SiO_2 substrate [22, 27].

We propose a model to qualitatively explain the above gate-polarity-dependent doping effect of H_2O-adsorption on

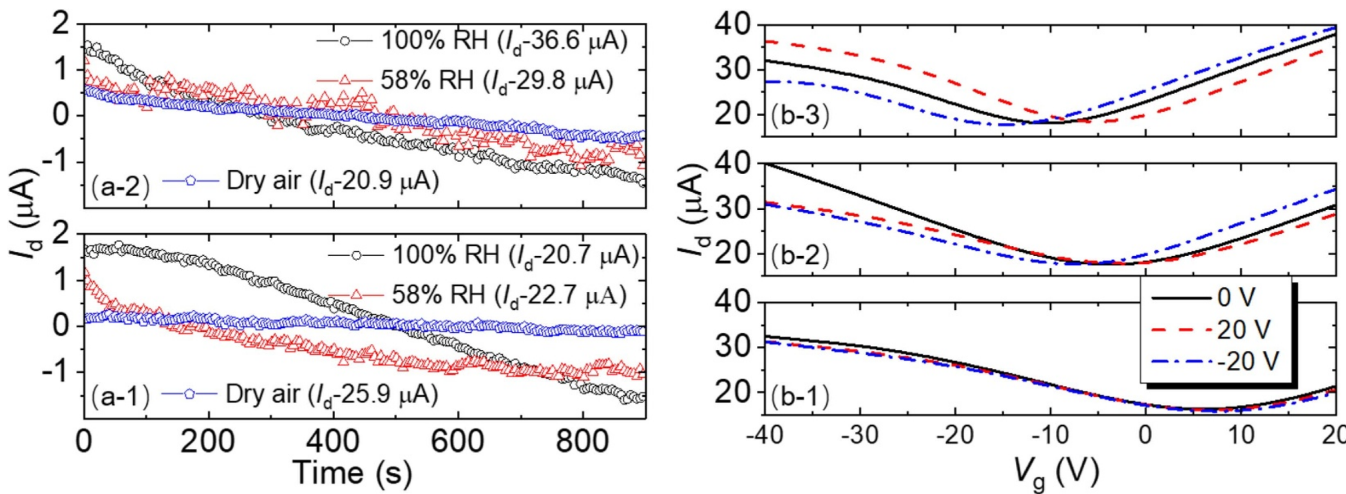

Figure 3. (a) Source-drain currents with respect to time (0–900 s) of the GFET in dry air (0% RH) and atmospheric conditions with 58% and 100% RH at 300 K, (a-1) and (a-2) for gate voltages of 20 V and −20 V, respectively. The source-drain bias voltage is set to 0.1 V. Before each of the above measurements, the device is kept for 30 min in the atmospheric conditions with 0% RH (dry air), 58% RH, and 100% RH, respectively. (b) Transfer curves measured at once after the measurements of the corresponding current–time curves shown in (a), (b-1) in 0% RH, (b-2) 58% RH, and (b-3) 100% RH.

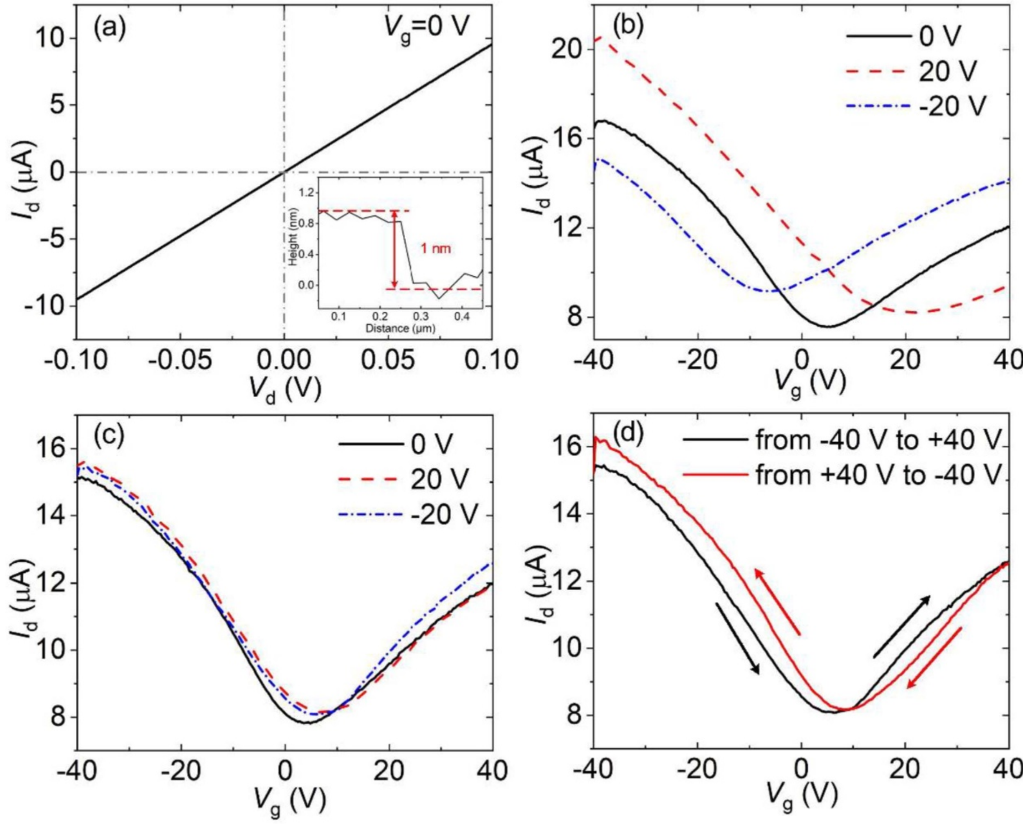

Figure 4. (a) The output characteristic of the few-layer GFET at $V_g = 0$ V. Transfer curves measured at once after the measurements of the corresponding current–time curves under different gate voltages in the atmospheric condition with 58% RH (b) and in the vacuum environment (c). (d) Transfer characteristic of the GFET in vacuum condition, acquired along two different gate voltage sweep directions.

graphene. The charge transfers between adsorbates and graphene is dependent on the orientation of the adsorbed molecules [7]. Generally speaking, p-type doping is achieved by adding atoms with fewer valence electrons than carbon, while n-type doping is generally achieved by adding atoms with more valence electrons than carbon [28]. Therefore, the fact of n doping of H_2O adsorption on graphene indicates that the O atom towards the graphene layer is the preferred orientation of the adsorbed H_2O molecules [7]. On the other hand, the very small effective charge transfer per H_2O molecule means

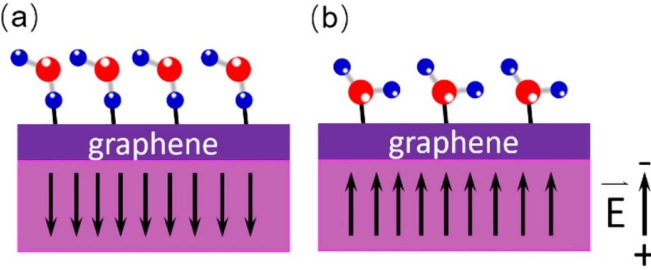

Figure 5. Schematics of gate-polarity-induced orientations of the adsorbed H_2O molecules at positive gate voltage (a) and negative gate voltage (b).

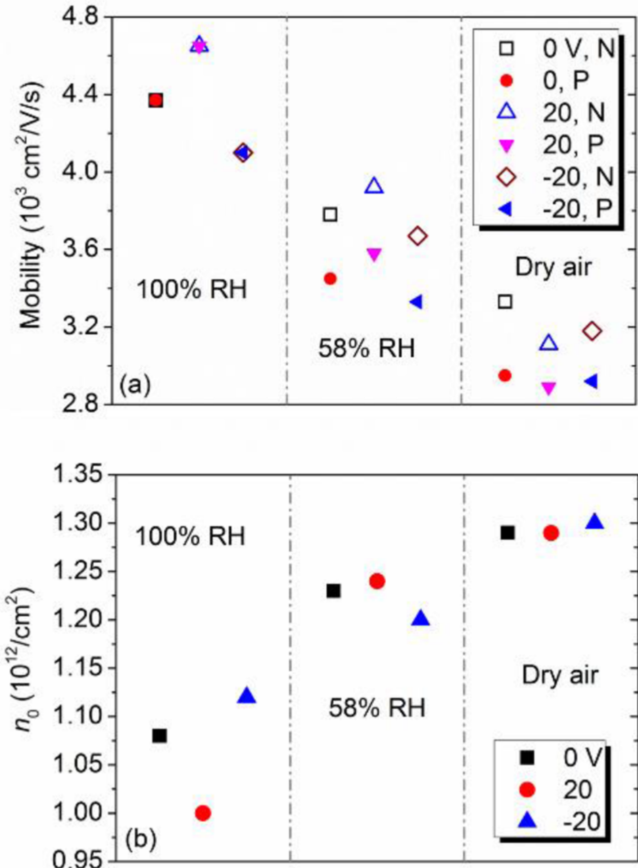

Figure 6. Theoretical fitting of experimental transfer-curve data based on the drift–diffusion model, the derived carrier mobilities (a) and the residual carrier concentrations (b) in atmospheric conditions with dry air (0% RH), 58% RH, and 100% RH, respectively.

that the orientations of adsorbed H_2O molecules are very close to randomness [6]. As shown in figure 5, the gate voltages will change the relative electrical potential of the graphene–SiO_2 interface. For positive gate voltages, as shown in figure 5(a), H atoms toward the graphene layer are the preferred orientations of the adsorbed H_2O molecules and the electron transfer is from the graphene layer to the adsorbed H_2O molecules. On the contrary, for negative gate voltages, O atoms toward the graphene layer are preferred orientations and the direction of electron transfer is reversed as shown in figure 5(b).

There is another possible mechanism to be responsible for the gate-polarity-dependent doping behavior of the adsorbed H_2O molecules. Instead of the change of adsorption orientation, the adsorption/desorption rates can be changed by the gate voltages, which will result in the change of doping behavior of H_2O adsorbates. The experimental data for the O_2 adsorption in dry air (figure 3(b-1)) indicate that the adsorption/desorption rates are not evidently influenced by the gate voltage. The adsorption energies for H_2O and O_2 adsorbates on graphene are in the range of ~47 meV [5]. If the adsorption/desorption rates are mainly determined by the adsorption energy, the gate-polarity-induced change of adsorption orientation may be the preferred mechanism responsible for the change of doping behavior of H_2O adsorbate. Further experiments are necessary to identify which mechanism plays the dominant role.

By using the drift–diffusion transport model (equation (1)), the experimental data are fitted with the electron and hole mobilities μ and the residual carrier concentration n_0 as the free parameters. The derived values of μ and n_0 in different ambient environments are depicted in figure 6. With the increase of RH, the carrier mobilities increase and the residual carrier concentration decreases, which can be explained by the fact that the screening of H_2O adsorptions reduces the negative effects of defects on the interface of graphene–SiO_2 on the carrier transport in the graphene channel. The gate voltages have no essential influence on the above parameters.

4. Conclusion

In summary, GFETs/SiO_2 are fabricated by using the mechanically exfoliated multilayer/few-layer graphene flakes as conductive channels. Gate-polarity-dependent doping behaviors of H_2O adsorption on the channel of GFETs/SiO_2 are experimentally investigated. In vacuum, there is no trapped-carrier-induced hysteretic behavior in the I_d–V_g transfer curves. In different atmospheric conditions (0% RH, 58% RH, and 100% RH) and at the temperature of 300 K, the dependences of the CNPs on the gate-voltage polarities are measured. When the GFET is negatively (−20 V), zero, and positively (20 V) gated, respectively, in the atmospheric conditions of 58% RH and 100% RH for 30 min, the CNPs on the transfer curves shift to right along the gate voltage axis. However, if the GFET is operated in vacuum and in dry air, respectively, the CNPs do not shift. We propose a model to explain the experimental results that the orientation of the adsorbed H_2O molecules can be affected by the gate-voltage polarity due to the dipolar interaction. For positive gate voltages, the orientation of H atom towards graphene is the preferred configuration, and the H_2O adsorbates in such an orientation behave as acceptors. For negative gate voltages, the orientation of O atom towards graphene is the preferred configuration, and the H_2O adsorbates in such an orientation behave as donors. The influence of graphene thickness is investigated. With reducing the thickness of graphene, the amphoteric doping behavior of H_2O adsorption is more sensitive to the gate voltage polarity.

Acknowledgments

This work was supported in part by the National Natural Science Foundation of China (61731020, 61722111), the National Key Research and Development Program of China (2017YFA0701005), the 111 Project (D18014), the International Joint Lab Program supported by Science and Technology Commission Shanghai Municipality (17590750300), and the Young Yangtse River Scholar (Q2016212).

ORCID iDs

Xuguang Guo https://orcid.org/0000-0003-1733-6478
Anqi Yu https://orcid.org/0000-0003-4615-8025

References

[1] Neto A C, Guinea F, Peres N M, Novoselov K S and Geim A K 2009 *Rev. Mod. Phys.* **81** 109
[2] Wallace P R 1947 *Phys. Rev.* **71** 622
[3] Meng Z, Stolz R M, Mendecki L and Mirica K A 2019 *Chem. Rev.* **119** 478–598
[4] Schedin F, Geim A K, Morozov S V, Hill E, Blake P, Katsnelson M I and Novoselov K S 2007 *Nat. Mater.* **6** 652–5
[5] Melios C, Giusca C E, Panchal V and Kazakova O 2018 *2D Mater.* **5** 022001
[6] Kong L, Enders A, Rahman T S and Dowben P A 2014 *J. Phys.: Condens. Matter.* **6** 443001
[7] Yang Y and Murali R 2011 *Appl. Phys. Lett.* **98** 093116
[8] Wehling T O, Lichtenstein A I and Katsnelson M I 2008 *Appl. Phys. Lett.* **93** 202110
[9] Leenaerts O, Partoens B and Peeters F 2009 *Phys. Rev.* B **79** 235440
[10] Böttcher S, Vita H, Weser M, Bisti F, Dedkov Y S and Horn K 2017 *J. Phys. Chem. Lett.* **8** 3668–72
[11] Lu J Y, Olukan T, Tamalampudi S R, Al-Hagri A, Lai C Y, Al Mahri M A, Apostoleris H and Chiesa M 2019 *Nanoscale* **11** 7944–51
[12] Melios C, Winters M, Strupiński W, Panchal V, Giusca C E, Jayawardena K I, Rorsman N, Ravi P, Silva S and Kazakova O 2017 *Nanoscale* **9** 3440–8
[13] Hong G, Han Y, Schutzius T M, Wang Y, Pan Y, Hu M, Jie J, Sharma C, Müller U and Poulikakos D 2016 *Nano Lett.* **16** 4447–53
[14] Melios C, Centeno A, Zurutuza A, Panchal V, Giusca C E, Spencer S, Silva R P and Kazakova O 2016 *Carbon* **103** 273–80
[15] Hu H, Yang X, Guo X, Khaliji K, Biswas S R, de Abajo F J G, Low T, Sun Z P and Dai Q 2019 *Nat. Commun.* **10** 1–7
[16] Smith A D, Elgammal K, Niklaus F, Delin A, Fischer A C, Vaziri Forsberg S F, Rasander M, Hugosson H and Bergqvist L 2015 *Nanoscale* **7** 19099–109
[17] Park J, Kim D W, Woo J Y, Lee J and Han C S 2015 *J. Phys. D: Appl. Phys.* **48** 455102
[18] Hong Y, Wang S, Li Q, Song X, Wang Z, Zhang X, Besenbacher F and Dong M 2019 *Nanoscale* **11** 19334–40
[19] Lee M J, Choi J S, Kim J S, Byun I S, Lee D H, Ryu S, Lee C and Park B H 2012 *Nano Res.* **5** 710–7
[20] Strzelczyk R, Giusca C E, Perrozzi F, Fioravanti G, Ottaviano L and Kazakova O 2017 *Carbon* **122** 168–75
[21] Ni Z, Wang Y, Yu T and Shen Z 2008 *Nano Res.* **1** 273–91
[22] Wang H, Wu Y, Cong C, Shang J and Yu T 2010 *ACS Nano* **4** 7221–8
[23] Zhang Y, Brar V W, Girit C, Zettl A and Crommie M F 2009 *Nat. Phys.* **5** 722–6
[24] Martin J, Akerman N, Ulbricht G, Lohmann T, Smet J V, Von Klitzing K and Yacoby A 2008 *Nat. Phys.* **4** 144–8
[25] Solís-Fernández P, Okada S, Sato T, Tsuji M and Ago H 2016 *ACS Nano* **10** 2930–9
[26] Li H, Han X, Childress A S, Rao A M and Koley G 2019 *Physica* E **107** 96–100
[27] Unarunotai S, Murata Y, Chialvo C E, Kim H S, MacLaren S, Mason N, Petrov I and Rogers J A 2009 *Appl. Phys. Lett.* **95** 202101
[28] Liu H, Liu Y and Zhu D 2011 *J. Mater. Chem.* **21** 3335–45